Glassy properties and viscous slowing down: An analysis of the correlation between nonergodicity factor and fragility

Kristine Niss,[1,2,a)] Cécile Dalle-Ferrier,[1] Valentina M. Giordano,[3] Giulio Monaco,[3] Bernhard Frick,[4] and Christiane Alba-Simionesco[1]
[1]*Laboratoire de Chimie Physique, Bâtiment 349, Université Paris-Sud, 91405 Orsay, France*
[2]*DNRF Centre "Glass and Time," IMFUFA, Department of Sciences, Roskilde University, Roskilde, 2000, Denmark*
[3]*ESRF, BP 220, 6 Rue Jules Horowitz, 38043 Grenoble, France*
[4]*Institut Laue-Langevin, BP 156, 6 Rue Jules Horowitz, 38042 Grenoble, France*

(Received 23 June 2008; accepted 30 September 2008; published online 20 November 2008)

We present an extensive analysis of the proposed relationship [T. Scopigno *et al.*, Science **302**, 849 (2003)] between the fragility of glass-forming liquids and the nonergodicity factor as measured by inelastic x-ray scattering. We test the robustness of the correlation through the investigation of the relative change under pressure of the speed of sound, nonergodicity factor, and broadening of the acoustic exitations of a molecular glass former, cumene, and of a polymer, polyisobutylene. For polyisobutylene, we also perform a similar study by varying its molecular weight. Moreover, we have included new results on liquids presenting an exceptionally high fragility index m under ambient conditions. We show that the linear relation, proposed by Scopigno *et al.* [Science **302**, 849 (2003)] between fragility, measured in the liquid state, and the slope α of the inverse nonergodicity factor as a function of T/T_g, measured in the glassy state, is not verified when increasing the data base. In particular, while there is still a trend in the suggested direction at atmospheric pressure, its consistency is not maintained by introducing pressure as an extra control parameter modifying the fragility: whatever is the variation in the isobaric fragility, the inverse nonergodicity factor increases or remains constant within the error bars, and one observes a systematic increase in the slope α when the temperature is scaled by $T_g(P)$. To avoid any particular aspects that might cause the relation to fail, we have replaced the fragility by other related properties often evoked, e.g., thermodynamic fragility, for the understanding of its concept. Moreover, we find, as previously proposed by two of us [K. Niss and C. Alba-Simionesco, Phys. Rev. B **74**, 024205 (2006)], that the nonergodicity factor evaluated at the glass transition qualitatively reflects the effect of density on the relaxation time even though in this case no clear quantitative correlations appear. © *2008 American Institute of Physics*. [DOI: 10.1063/1.3005646]

I. INTRODUCTION

A fundamental question in condensed matter science is to understand what governs the increase in relaxation time and ultimately the glass formation at a temperature T_g in liquids upon cooling. This increase in relaxation time upon cooling is not specific to a glass forming system but is universal in the sense that it regards all types of materials ranging from metals to polymers and proteins. However, the relaxation time has quantitatively different temperature dependencies from one system to another. This difference can be quantified via the "fragility," which is a measure of departure from an Arrhenius temperature dependence of the viscosity as the temperature decreases. The fragility concept has become widely used in the community because it captures the notion of universal and specific at the same time, and offers a criterium for ranking or classifying systems of all types. On one hand, there is something universal we want to understand, namely, the viscous slowing down, particularly the super-Arrhenius temperature dependence of the relaxation time as T_g is approached. However, there is something specific to each system that we need to capture—all is embodied in the fragility. In other words, a crucial question to address in the field—"what controls the viscous slowing down?"—can therefore be rephrased as "what governs the fragility of a system and makes it system dependent?"

Because of the rich phenomenology related to the glass formation, a lot of experimental efforts has been put within the past decade into correlating fragility with different properties of the liquid and the glass in order to extract the central components that should be included in a theory. In particular, it was suggested that the differences observed in the vibrational properties, harmonic and anharmonic contributions of glasses, could originate from the variations in the fragility of the supercooled liquids from which the glasses were formed. Accordingly, the legitimate question to address becomes how the T-dependence of the relaxation time of a liquid is embedded in the properties of its glass as proposed by Scopigno *et al.*[1] It appears that glassy or short time dynamics (at the pico-nanosecond time scale) could be related to the viscous slowing down of the liquid at some second time scale. This statement is based on striking empirical results reported in

[a)]Electronic mail: kniss@ruc.dk.

literature over the past decade.[1–8] A number of these results (and earlier related results) are reviewed and combined by Dyre.[9,10] Also, Novikov *et al.*[2,11] discussed a variety of this type of results and suggested that they are intimately connected to each other. In this paper, we specifically focus on the proposed relation between the fragility measured in the supercooled liquid close to the glass transition temperature T_g and the low-temperature dependence of the inverse nonergodicity factor in the glass as determined from inelastic x-ray scattering (IXS) as a function of T/T_g.[1] The nonergodicity factor f_Q is defined as the plateau value reached by the normalized density-density correlation function; it characterizes the amplitude of the structural relaxation or α-process at a given wave number Q and, taken at T_g, it characterizes the amplitude of the structural relaxation or α-process. Above T_g, the time scale at which the f_Q is measured must be shorter than the relaxation time. The f_Q reflects how correlated the density-density fluctuations are in the supercooled liquid until the function decreases to zero and its temperature dependence is well described by the mode coupling theory. At T_g, the fluctuations are frozen on the experimental time scale and, consequently, ergodicity is macroscopically broken; in the glass below T_g,f_Q increases as temperature decreases and reflects the temperature dependence of the relative contribution of the elastic scattering to the total scattered intensity.

The studies of the abovementioned questions and conjectures have traditionally, and in some cases almost solely, been performed by comparing the temperature dependence of the dynamics in different glass formers, i.e., by associating the fragility with the chemical structure of the system. However, other control parameters can be considered to tune the fragility without modifying the chemical interactions. Typically, pressure is a control variable, adjoined to the temperature, that allows one to extract new information because it leads to a continuous change in T_g, density, and fragility. Pressure was used as an additional parameter to study the correlation found in Ref. 1 in a molecular dynamics simulation by Ribeiro *et al.*[12]—but experimental tests have not, to our knowledge, been reported elsewhere. The introduction of pressure allows for a more systematic test of a correlation; moreover, it facilitates the disentanglement between temperature and density contributions in the phenomenon. The introduction of pressure leads to the natural consideration of the *isochoric* fragility, m_ρ, in addition to the classical *isobaric* fragility, m_P. Two of us have earlier shown how this leads to a number of consequences, which can be useful when analyzing different correlations or relations between fragility and other properties.[13,14]

There is a special class of systems for which similar arguments can be developed, polymers. They are often evoked in the search of correlation since in many respects their glass formation at the segmental scale looks like the one of molecular liquids. Over the past years, we have examined several features of glasses at the segmental scale and the glass transition (e.g., Refs. 15–19). Studying polymers presents an appreciable advantage over molecular liquids, since an extra control parameter, changing the chain length by modulating the number of monomers, can be introduced without altering the enthalpic interaction parameters. Thus, the properties of the system, e.g., T_g, density, and fragility, can be modified by changing the molecular weight M_w of the polymer, which can be, in this sense, considered as an additional control parameter analogous to pressure. It provides a sensitive tool for a more systematic evaluation of the different relations that have been suggested between properties in glass forming systems and glasses. Moreover, polymers are easily compressed and the lines of reasoning cited above can be applied.

In the viewpoint of testing correlations, extreme cases are always good to include and liquids of exceptionally high fragility, in the limit of the order of 170,[20] are of special interest. However, one should verify in these cases what ranks them as extremes and consider here correlation to isochoric fragility as well as, to isobaric fragility since the latter relates to both density and temperature effects. This view is supported by an experimental work showing that the isobaric fragility depends on pressure, whereas the isochoric fragility is independent of density,[14,21–24] a result which strongly suggests that the isochoric fragility is an intrinsic property of the liquid.

We have studied the temperature dependence of the coherent dynamical structure factor measured by IXS in the molecular glass-former cumene and polyisobutylene (PIB) at atmospheric pressure and at 300 MPa. In the case of PIB, we have additionally considered its molecular weight dependence by including samples of three distinct M_w. Moreover, we include in our analysis the ultrafragile molecular liquid decahydroisoquinoline (DHIQ) and the fragile sorbitol. The latter is also an interesting extreme case of a system where the relaxation time is very weakly dependent on density, which, in turn, means that m_p is close to m_ρ.

Concomitant to the change in fragility, we focus our attention on the subsequent variations in the nonergodicity factor and scrutinize with great care the correlation proposed in Ref. 1. In particular, we put these new results within a framework where the role of density on the viscous slowing down was demonstrated to be crucial for understanding them.[13] To overcome specific aspects that might cause the failure of the correlation, especially the great variation found in literature in quantifying the fragility (distributed over 20% up to 50%), we have considered other quantities often evoked in its definition or associated to it. Since thermodynamics and kinetics are often proposed to be linked, we extend our analysis to the thermodynamic fragility and quantities involved in its definition according to a theoretical model[25,26] or empirical relations.[20]

This paper is structured as follows. In Sec. II, we present the details of the experiments, samples, and data treatment. The results in terms of the speed of sound, broadening of the acoustic excitation, and the nonergodicity factor are presented in Sec. III including pressure, M_w effects, and thermodynamic considerations. In Sec. IV, we use our results to consider different relations suggested between high frequency properties of the glass or liquid and the viscous slowing down, particularly between the isobaric fragility and the temperature dependence of the nonergodicity factor,[1] between the nonergodicity factor at T_g and the effect of density

TABLE I. The glass transition temperatures are considered at 1000 s in general and at 100 s for DHIQ and sorbitol.

Sample	T_g (K)	m_P	dT_g/dP (K MPa^{-1})
Cumene	126	90[a]	0.07[b]
DHIQ	180[c]	158[d]	
Sorbitol	273	100[e]	
PIB680	189	80[a]	0.06
PIB3580	195		0.067
PIB500k	204	46[f]	0.164

[a]Reference 30.
[b]Reference 52.
[c]Reference 53.
[d]Reference 54.
[e]Reference 55.
[f]Reference 56.

on the viscous slowing down,[13] and between the isobaric fragility and the broadening of the acoustic excitation.[27] The conclusions are summarized in Sec. V.

II. EXPERIMENTAL SECTION

A. IXS experiments

The IXS experiments on cumene, sorbitol, and DHIQ were performed on the IXS beamline ID16 at the ESRF, while the experiment on PIB was performed on ID28.

1. Samples

Cumene was purchased from Fluka at a purity of 99.5%. DHIQ (96%) is a *cis-trans* mixture and was obtained from Aldrich. D-sorbitol (97%) was purchased from Aldrich. They were all conditioned in a glovebox with no further purification. The polymeric samples used are PIB680, PIB3580, and PIB500k. PIB680 (M_w=680 g/mol, M_w/M_n=1.06) and PIB3580 (M_w=3580 g/mol, M_w/M_n=1.23) are from Polymer Standard service, PIB500k (M_w=500.000 g/mol, M_w/M_n=2.5) is from Sigma Aldrich. See Table I for T_g-values and fragilities.

2. Sample environment

The PIB, cumene, and DHIQ samples were placed in a 10 mm (or 20 mm) long cylindrical pressure cell, which was sealed at both ends by 1 mm thick diamond windows. The pressure cell was housed in a vacuum chamber using Kapton as window material. The pressure was applied using a piston-and-cylinder device. The pressure was always imposed above the (pressure dependent) glass transition temperature, and cooling was done isobarically by adjusting the imposed pressure upon cooling.

TABLE II. The values used in Figs. 12–14 and their references. tw stands for "this work" and " *" denotes that the value is determined based on date in the reference ("+" dibutyl phtalate).

	m_P	m_V	f_Q (T_g)	α	Γ	x
Cumene	90[a]	57[b]	0.60[tw]	0.44[tw]	0.3[tw]	4.85[b]
Cumene 3 kbar	72*[c]	57[b]	0.63[tw]	0.58[tw]	0.3[tw]	4.85[b]
PIB 500k	46[d]	34[e]	0.65[tw]	0.55[tw]	1.10[tw]	2.60[e]
PIB 680	68[b]		0.85[tw]	0.173[tw]		
Salol	68[f]	36[g]	0.61*[h]	0.64[h]		5.20[i]
Glycerol	47[j]	38[k]	0.76[h]	0.32[h]	0.28[l]	1.60[m]
DBP+	75[n]	63[n]	0.86[o]	0.16*[o]	0.15[o]	1.70[n]
DBP 2 kbar	75[n]	63[n]	0.84[o]	0.18*[o]		2.70[n]
m-toluidine	82[p]	68[n]	0.68[q]	0.57[q]		2.30[n]
DHIQ	158[r]		0.77[tw]	0.23[tw]	0.3[tw]	3.55[s]
Sorbitol	100*[t]		0.74[tw]	0.36[tw]	0.3[tw]	0.13
o-TP	81[u]	45*[k]	0.63[h]	0.58[h]	0.25[w]	4.00[v]
o-TP 2 kbar	60*[k]	45*[k]	0.60[w]	0.66[w]	0.25[w]	4.00[v]
(1,4)-PB	60[h,k]	64[k]	0.71[x]	0.4[x]		
BeF_2			0.86[h]	0.16[h]		
Silica			0.84[h]	0.191[h]	1.33[l]	
n-BB			0.69[h]	0.46[h]		
m-TCP			0.63[h]	0.59[h]		
Se			0.59[h]	0.7[h]	0.23[l]	
GeO_2	28[l]				1.30[l]	
$ZnCl_2$	45[l]				0.58[l]	

[a]Reference 57.
[b]Reference 30.
[c]References 57–60.
[d]Reference 56.
[e]Reference 29.
[f]References 40, 61, and 62.
[g]Reference 63.
[h]Reference 1.
[i]Reference 40.
[j]References 64 and 65.
[k]Reference 64.
[l]Reference 27.
[m]References 44 and 64.
[n]Reference 14.
[o]Reference 42.
[p]References 66 and 67.
[q]Reference 68.
[r]Reference 54.
[s]Reference 69.
[t]Reference 55.
[u]References 62, 64, 70, and 71.
[v]References 64, 72, and 73.
[w]Reference 41.
[x]Reference 74.

The experiment on PIB was performed using ethanol as pressurizing medium. Ethanol does not dissolve PIB easily in these conditions. We isolated the sample from the ethanol by placing it in a 9.9 mm long Teflon cylinder closed in both ends with a Teflon film. The Teflon cell was subsequently mounted on the pressure cell.

The experiment on cumene was performed using the cumene itself as pressurizing medium. The experiment on DHIQ was performed with DHIQ placed in a 9.9 mm long aluminium capsule, mounted on the pressure cell. The experiment on sorbitol was realized in a standard cell for atmospheric pressure experiment, a glass cell with diamond windows.

3. Experiment on molecular liquids

The (11 11 11) [and (12 12 12) for sorbitol] reflection of the Si monochromator and analyzer crystals was used for the reported experiments yielding an energy resolution of full width at half maximum (FMHW)=1.5 meV (and 1.3 meV, respectively).[28]

The dynamical structure factor of cumene was recorded at different temperatures in the glass and in the liquid at atmospheric pressure and at 300 MPa. The analyzers were set to give the Q-values of 2, 1, 4, 7, and 10 nm^{-1}. The integration time per point was minimum of 180 s and was increased by a factor 2 or 3 at lower temperatures where the inelastic intensity is lower. DHIQ was studied only at atmospheric pressure with the same Q-setting.

Sorbitol was studied at a higher resolution with a different Q-settings: 1.2, 2, 4.5, 7.9, and 11 nm^{-1}.

4. Experiment on PIB

The (11 11 11) reflection of the Si monochromator and analyzer crystals was used for the reported experiments yielding an energy resolution of FMHW=1.5 meV.[28] We measured the dynamical structure factor as a function of temperature at atmospheric pressure for PIB samples with different molecular weights. The PIB680 and PIB3580 samples were moreover studied at 300 MPa. The Q settings 2, 5, 8, 11, and 14 nm^{-1} were used for all the samples under all P-T conditions. Several additional Q settings were used at some conditions. The integration time per point was 70 s.

5. Calorimetric data

The calorimetric glass transition line $T_g(P)$ for τ_α of 10^3 s was previously determined by using a high precision calorimetric device for PIB (Ref. 29) and estimated from dielectric experiments and literature viscosity data for cumene.[30]

B. Data treatment

The data are fitted by using of a damped harmonic oscillator for the inelastic signal and a delta function $\delta(\omega)$ for the elastic line

$$\mathcal{S}(Q,\omega) = \mathcal{S}(Q)\left(f(Q)\delta(\omega) + [1 - f(Q)]\frac{1}{\pi}\frac{\Omega^2\Gamma(Q)}{(\omega^2 - \Omega^2(Q))^2 + \omega^2\Gamma^2(Q)}\right). \quad (1)$$

The normalization of the functions ensures that $\int S(Q,\omega)d\omega = S(Q)$ and $f(Q)$ gives the nonergodicity factor at a given momentum transfer Q. The associated wavelength is $2\pi/Q$, Ω gives the frequency of the mode in question, and Γ denotes its broadening (FWHM). The above function is symmetric in energy transfer ω. Detailed balance is obtained by multiplying with the factor $\omega/(k_BT)/(1-\exp(-\omega/(k_BT)))$. The last point of the analysis is the convolution with the resolution function. The resolution is obtained experimentally at the beamline by the measurement of a Plexiglass sample at the structure factor maximum and at low temperatures, where the inelastic signal is very small. The complete function used in the fitting procedure is, hence,

$$I(Q,\omega) = A\int R(\omega-\omega')\left(f(Q)\delta(\omega') + \frac{\omega'\beta}{1-\exp(-\omega'\beta)}[1 - f(Q)]\frac{1}{\pi}\frac{\Omega^2\Gamma(Q)}{(\omega'^2 - \Omega^2(Q))^2 + \omega'^2\Gamma^2(Q)}\right)d\omega'. \quad (2)$$

Here A is a factor that contains $S(Q)$ as well as the total number of scatterers, scattering length, etc., ω is the energy (in our case measured in meV), and $\beta = 1/k_BT$. The quality of the fits is generally very convincing; this is illustrated in Fig. 1.

In the PIB experiments under pressure we also had in the beam a thin Teflon film and possibly ethanol (between the Teflon and the diamond window). This gives rise to an elastic signal of the order of magnitude 10% of the total intensity of the sample. This empty cell signal, once reduced by the sample transmission, is subtracted from the measured elastic intensity. The subtraction of this empty cell contribution does not affect the determination of the position of the side peaks nor of their widths because it is purely elastic. However, it does influence the nonergodicity factor and leads to a relatively larger error on this quantity (this effect is included in the error bars shown in the figures).

III. RESULTS

In this section, we summarize the pressure effects on the acoustic speed, broadening, and on the nonergodicity factor for the three samples studied under pressure.

A. Pressure effects

1. Speed of sound

The effect of pressure is a shift of the Brillouin lines to higher frequency (Fig. 1), corresponding to an increase in the speed of sound. The shift corresponds to a change in the speed of sound from 2400 m/s at atmospheric pressure to 3400 m/s at 300 MPa for the PIB3580 at room temperature. This shift of the Brillouin lines and the related increase in the speed of sound are also illustrated in Fig. 2. This figure

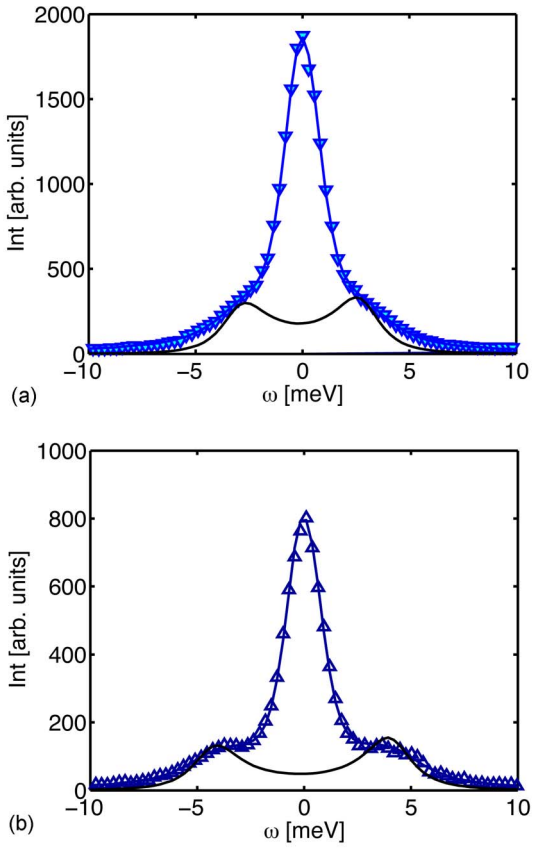

FIG. 1. (Color online) $S(Q,\omega)$ of PIB3580 at $Q=2$ nm^{-1} at room temperature, ambient pressure (left), and 300 MPa (right). The error bars are smaller than the symbols. The line through the data points illustrates the fit to Eq. (2). The double peaks illustrate the inelastic signal before convolution with the resolution function [second term of Eq. (1)].

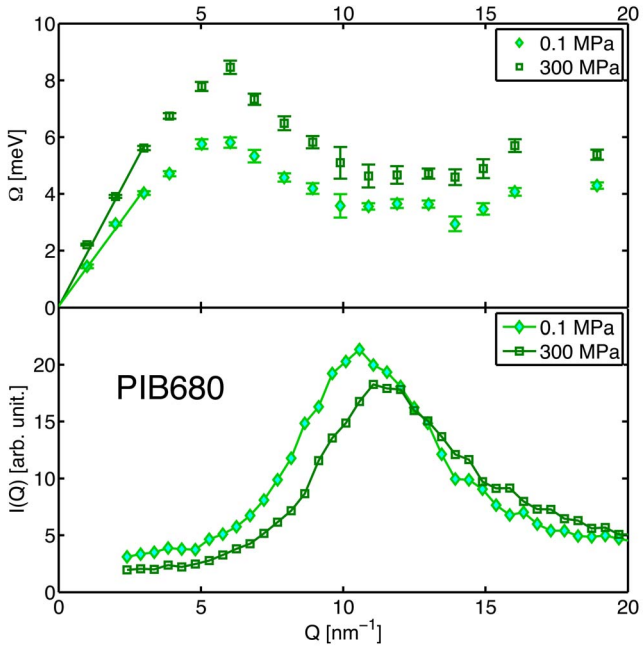

FIG. 2. (Color online) The upper figure shows the dispersion of longitudinal sound modes of PIB680 measured by IXS at room temperature, atmospheric pressure, and 300 MPa. The lower figure shows the total scattered intensity $I(Q)$ of PIB680 at room temperature, atmospheric pressure, and 300 MPa.

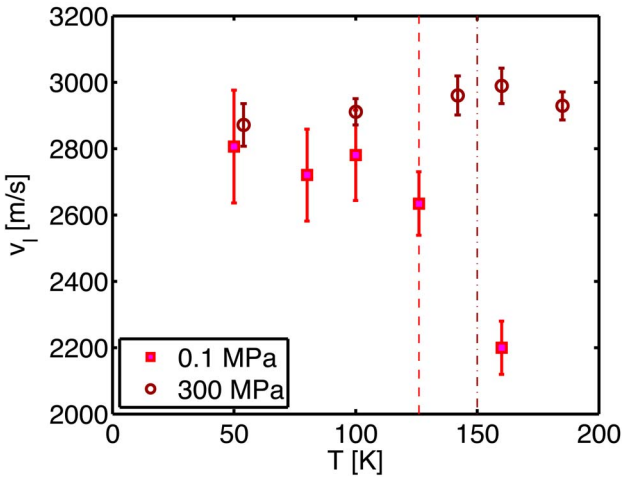

FIG. 3. (Color online) The dispersion of liquid cumene at $T=160$ K, ambient pressure, and at 300 MPa. The error bars are smaller than the symbols. The dashed lines are guides to the eye. $T_g(0.1\ \text{MPa})=126$ K and $T_g(300\ \text{MPa})=150$ K.

shows the dispersion of the sound modes in the Q-range from 2 to 20 nm^{-1} measured at ambient pressure and at 300 MPa for the PIB680 at room temperature. The qualitative behavior is the same at other temperatures and with samples of other molecular weights. The dispersion is linear up to $Q=3$ nm^{-1}, where it starts bending slowly off becoming flat around $Q=5$ nm^{-1}. This is similar to the dispersion curve generally seen for disordered materials,[31] showing a maximum at about $Q_m/2$, with Q_m as the position of the first structure factor maximum. $Q_m \approx 10$ nm^{-1} for PIB (Ref. 32) [the scattered intensity $I(Q)$ is also shown in Fig. 2]. While the data treatment remains quite successful at all Q's, the contribution of more than one excitation cannot be excluded especially at high Q's; thus as suggested by Bove *et al.*,[33] the combination of two damped harmonic oscillators could be meaningful. Therefore we limit our analysis to the lowest Q-range.

The qualitative behavior of the cumene dispersion and its pressure dependence is similar to that of PIB and of other systems[31] with a linear dispersion at low Q and a bend at around $Q_m/2$. The dispersion appears to stay linear in a longer range than in the case of PIB, being close to linear all the way up to 4 nm^{-1}, and bends after this (Fig. 3), although this is difficult to determine precisely in view of the relatively scarce number of points.

The speed of sound in the glass is temperature independent within error bars, while the speed of sound decreases when temperature is increased above T_g. This is illustrated by the data of PIB680 in Fig. 4 and for cumene in Fig. 5. The data of cumene show an interesting behavior: the speed of sound at 300 MPa is essentially temperature independent over the entire temperature range; moreover, the pressure dependence of the speed of sound in the glass is very weak if present at all.

2. Broadening of the acoustic exitations

In Fig. 6 we show Γ/Q^2 for cumene and PIB3580 as a function of temperature at atmospheric pressure as well as at

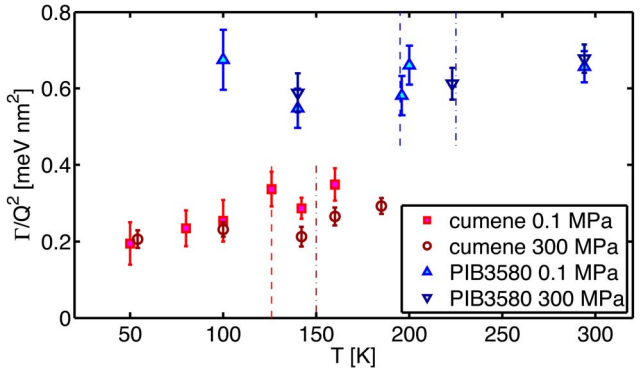

FIG. 4. (Color online) The speed of sound of PIB680 at room pressure and at 300 MPa as a function of temperature (calculated from the excitation at $Q=2$ nm^{-1}). The speed of sound in the glass is temperature independent within error bars, while the speed of sound decreases when temperature is increased above T_g. The dashed lines indicate the two glass transition temperatures. T_g(0.1 MPa)=190 K and T_g(300 MPa)=208 K. A similar behavior is found for PIB3580 (not shown).

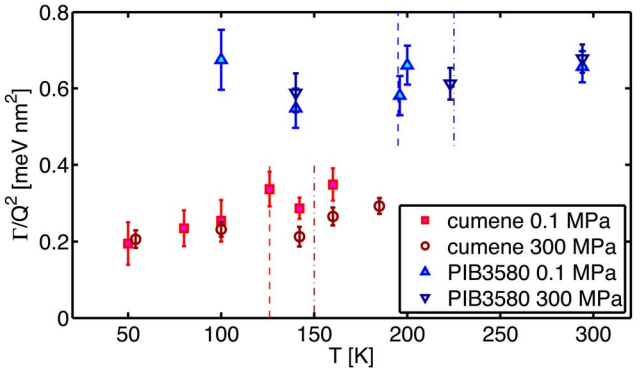

FIG. 6. (Color online) Γ/Q^2 of PIB3580 and cumene at atmospheric pressure and 300 MPa as a function of temperature. The data shown are taken at the highest available Q-value in the linear range of the dispersion curve; for PIB3580 at $Q=2$ nm^{-1}, while for the cumene data it is at $Q=4$ nm^{-1}. The dashed lines indicate the glass transition temperatures. For PIB3520 T_g(0.1 MPa)=195 K and T_g(300 MPa)=225 K. For cumene, T_g(0.1 MPa) =126 K and T_g(300 MPa)=150 K.

300 MPa. The relatively low speed of sound of the samples under consideration has the consequence that the Brillouin peaks are very close to the central line and, in some cases, almost buried under the tail of the resolution function. It is consequently more difficult to determine the broadening Γ. Within the error bars we find that the Γ for all the samples is independent of pressure and of temperature. As Γ/Q^2 (the quantity shown in Fig. 6) is independent of Q at low Q, the Q-dependence of the broadening of the acoustic excitation below the bend of the dispersion curve is consistent with a Q^2-dependence. However, the Q^2-dependence cannot be extracted independently from the data due to the relative scarce number of Q-values and the relative large error bars.

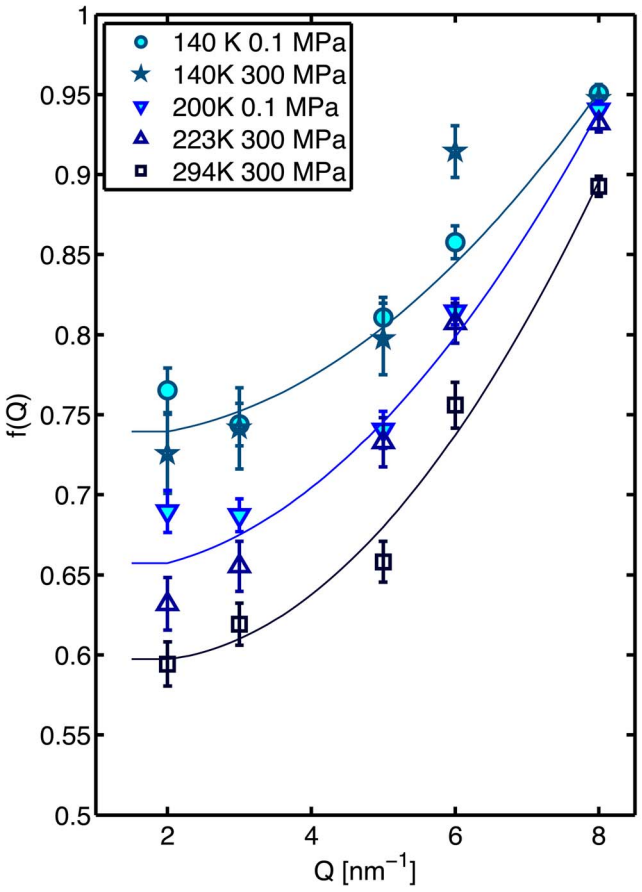

FIG. 5. (Color online) The speed of sound of cumene calculated at Q =2 nm^{-1} as a function of temperature at ambient pressure and at 300 MPa. The dashed lines indicate the glass transition temperatures. T_g(0.1 MPa) =126 K and T_g(300 MPa)=150 K.

3. Nonergodicity factor

The wave-vector dependence of the nonergodicity factor follows the expected oscillation with the $S(Q)$. That is, it is Q-independent in the low Q-region and increases when approaching the structure, factor maximum; this is illustrated with data of PIB3580 in Fig. 7. In the following we focus on the nonergodicity factor measured at $Q=2$ nm^{-1}.

It is clear directly from Fig. 7 that the temperature dependence of the nonergodicity factor dominates over the pressure dependence. In Fig. 8 we show the temperature dependence of the nonergodicity factor of PIB680, PIB3580, and cumene at different pressures. It is in all three cases seen that the nonergodicity factor shows the expected decrease with temperature. It is independent of pressure for $T<T_g$. In PIB3580 a weak decrease in the nonergodicity factor with increasing pressure at $T>T_g$ is seen, while the nonergodicity factor of cumene increases with increasing pressure in the temperature domain above T_g.

B. M_w dependence

In Fig. 9 raw spectra of PIB680 and PIB3580 are shown in order to illustrate the effect on $S(Q,\omega)$ of changing the molecular weight. Both spectra are taken at 140 K and 2 nm^{-1}. It is clearly seen that the relative intensity of the Brillouin peaks is stronger in the high molecular weight sample than in the low molecular sample in the case of PIB. We have found that the speed of sound increases with increasing molecular weight at ambient pressure and room temperature in the melt, while in the glass no M_w dependence remains.

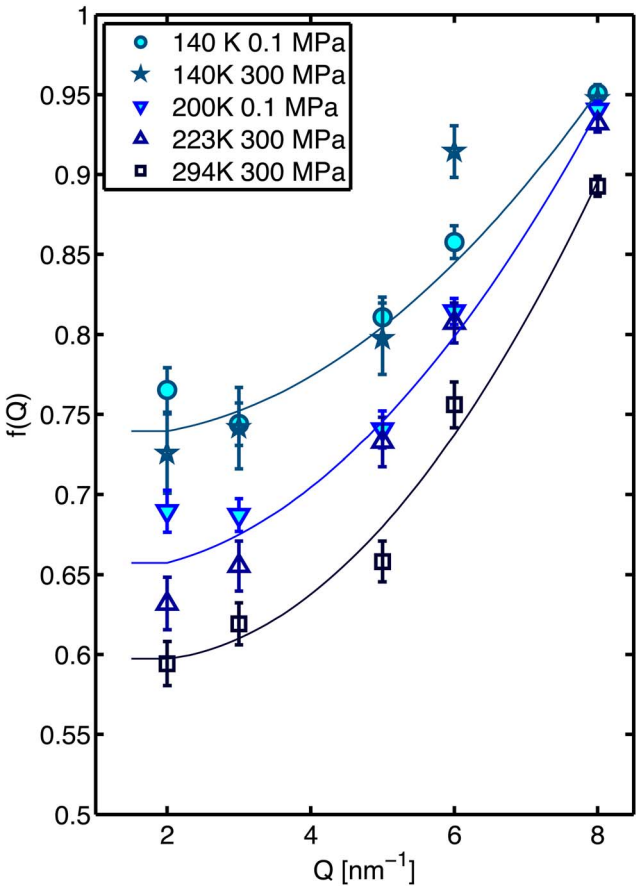

FIG. 7. (Color online) The nonergodicity factor, f_Q, as a function of Q for PIB3580 at different temperatures and pressures. It is seen that the Q-dependence is leveling off at low Q. Lines are guides to the eye.

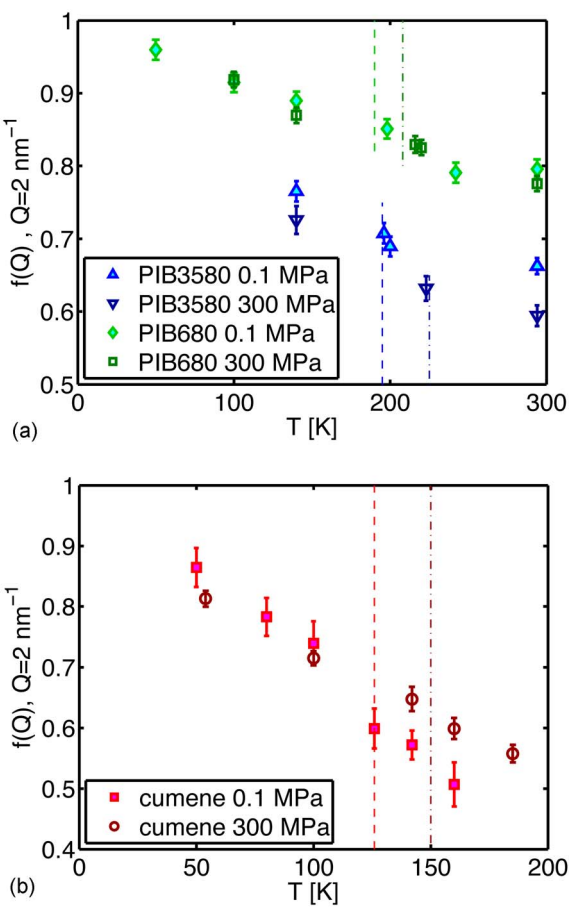

FIG. 8. (Color online) (a) The nonergodicity factor at $Q=2$ nm^{-1} of PIB680 and PIB3580 as a function of temperature at atmospheric pressure and 300 MPa. The dashed lines indicate the glass transition temperatures. For PIB680 $T_g(0.1\ \text{MPa})=190$ K and $T_g(300\ \text{MPa})=208$ K and for PIB3580 $T_g(0.1\ \text{MPa})=195$ K and $T_g(300\ \text{MPa})=225$ K. (b) Nonergodicity factor of cumene as a function of temperature at atmospheric pressure and 300 MPa at $Q=2$ nm^{-1}. The dashed lines indicate the glass transition temperatures of cumene $T_g(0.1\ \text{MPa})=126$ K and $T_g(300\ \text{MPa})=150$ K.

The low speed of sound and the low intensity of the Brillouin peaks of the low molecular sample, PIB680, had the consequence that we needed to fix the parameter Γ in order to get a stable DHO fit of the spectra. We have therefore not been able to determine the molecular weight dependence of Γ.

The influence of the molecular weight on the nonergodicity factor is quite strong for PIB. The nonergodicity factor is considerably larger for the low molecular weight. This is true for all temperatures and pressures. The difference is illustrated in Fig. 8, which shows the temperature dependence of the nonergodicity factor of PIB680 and PIB3580 at atmospheric pressure and $Q=2$ nm^{-1}. These results fit well with previous work on the M_w dependence of glassy properties of PIB.[19] New experiments are in progress to get a definite answer on the amplitude and the direction of these effects by adding more data at different M_w and comparing with another polymer, polystyrene.[34]

The increase in molecular weight and the increase in pressure both lead to an increase in the density and a decrease in the compressibility of the sample. It is also seen that the increase in M_w and the increase in pressure have the same qualitative effect on the speed of sound of the sample, namely, that the speed of sound increases in both cases. One could thus suspect that density could be the underlying parameter governing both the dependences on pressure and on molecular weight. However when we compare the quantitative behavior, we find a difference. As an example we consider the effect of the molecular weight and of pressure on the speed of sound of PIB at room temperature.

At room temperature for PIB, $M_w=3580$ g/mol^{-1} going from atmospheric pressure to 300 MPa leads to 10% increase in density ρ and 39% increase in the speed of sound v. This corresponds to a Grüneisen parameter $(d\log v/d\log\rho)$ of 3.9.

If the effect of the molecular weight could be explained solely by the change in density which is associated with the change in molecular weight, then we should be able to predict the molecular weights influence on the speed of sound from the Grüneisen parameter and the molecular weight dependence of density.

When going from $M_w=680$ to $M_w=500\,000$, we achieve 4% increase in density and the prediction based on the Grüneisen parameter (3.9) is therefore an increase in the speed of sound of 14%. In the experiment we find that the actual increase in the speed of sound is 23%. This clearly shows that the effect of changing the molecular weight is larger than the mere effect due to density changes.

In the glassy phase moreover we find that pressure has a

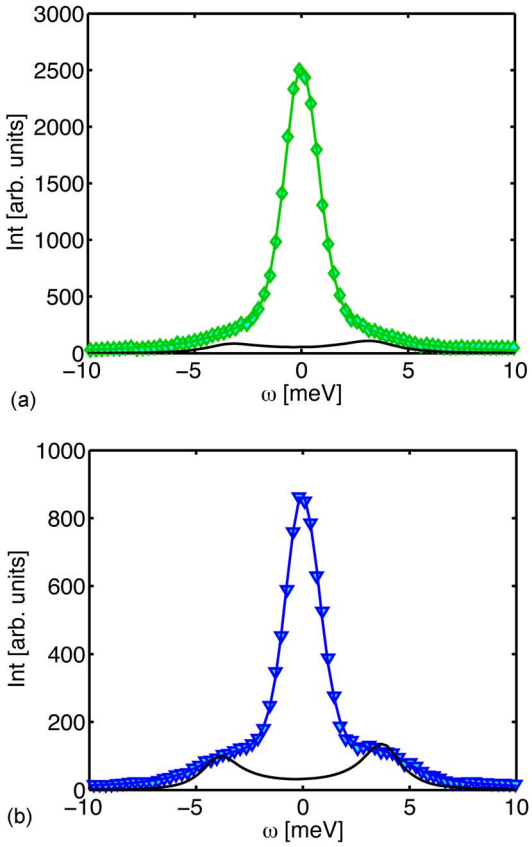

FIG. 9. (Color online) Illustration of how $S(Q,\omega)$ depends on the molecular weight. The left figure shows a spectrum of PIB680 and the right figure shows PIB500k. Both spectra are taken at 140 K and 2 nm^{-1}. The lines through the fit illustrate the fit to Eq. (2). The double peaks illustrate the inelastic signal before convolution with the resolution function [second term of Eq. (1)].

significant influence on the speed of sound in the PIB samples, while we find that the change in molecular weight has an insignificant effect on the speed of sound measured in the glassy samples even though density is increased with increasing the molecular weight.

Another parameter that clearly shows a difference between the effect of pressure and molecular weight is the change in f_Q. While f_Q at fixed temperature is almost pressure independent, it is strongly molecular weight dependent (see Fig. 8).

C. Nonergodicity factor and compressibility

In an equilibrium liquid, the low Q limit of $S(Q)$ is given by $k_BT\rho\kappa_T$. This result is based on the fluctuation dissipation theorem, which relates the density fluctuations to the response function κ_T. In the energy dependent $S(Q,\omega)$, the compressibility contribution is split into two parts. One is the central line that contains the density fluctuations that are frozen on the experimental time scale (given by the width of the resolution) that is the relaxational part of the compressibility. The other part is due to the fluctuations, which vary at frequencies corresponding to the sound modes at the studied Q-value; these contribute too in the Brillouin lines. The fast density fluctuations correspond to the acoustic excitations and the compressibility related to these also governs the longitudinal speed of sound, v_l. This leads to the following relations, where I is the measured intensity and A is a factor that contains the total number of scatterers, the form factor, etc.,

$$\lim_{Q\to 0} \mathcal{S}(Q) = k_BT\rho\kappa_T, \tag{3}$$

$$\lim_{Q\to 0} AI_{\text{tot}}(Q) = T\rho\kappa_T, \tag{4}$$

$$\lim_{Q\to 0} AI_{\text{inel}}(Q) = \frac{T}{v_l^2}. \tag{5}$$

The above observation is equivalent to the well known result[7,35]

$$f_Q = 1 - \frac{1}{\rho\kappa_T v_l^2}. \tag{6}$$

The relation between compressibility and intensity of the dynamic structure factor holds in the low Q limit, while the measurements are performed at a rather high Q-value, meaning that it is not *a priori* expected to find agreement with the IXS data. $Q=2$ nm^{-1} is, on the other hand, in the region where $S(Q)$ and f_Q approach their low Q plateaus and the dispersion curve is still linear in this range. This observation suggests that an agreement with the long wavelength behavior can be anticipated even in this region.

There are *PVT* equations available in literature for high molecular weight PIB (Ref. 36) (valid well above T_g). These data give access to the isothermal compressibility κ_T and make it possible to check Eq. (6). Using the data of PIB3580, we find that the f_Q which is directly measured and the f_Q which is calculated from the speed of sound v_l (also taken from IXS data) and κ_T agree within 10%, with the general trend that the calculated value is lower than the directly measured value. We have, for instance, for PIB3580 room temperature and ambient pressure $f_{Q,\text{measured}}=0.66$ and $f_{Q,\text{calcuted}}=0.62$, while the corresponding values at 300 MPa is $f_{Q,\text{measured}}=0.60$ and $f_{Q,\text{calcuted}}=0.57$. The agreement is convincing and nontrivial which is particularly clear when one considers that the sound velocity itself changes by ~50% when going from atmospheric pressure to 300 MPa at room temperature.

The interpretation above is restricted to temperatures above T_g because density fluctuations are frozen in the glass and there is no longer a correspondence between the density fluctuations measured by scattering and the compressibility one would measure in a macroscopic experiment where the system is compressed. The macroscopic compressibility measured by volume changes as a function of applied pressure will, as other thermodynamic derivatives, be discontinuous at T_g. It is moreover ill-defined in the glass because the system is out of equilibrium and the values obtained will depend on the thermodynamic path. $S(Q)$, on the other hand, does not change abruptly when T_g is overcome and stays more or less constant in the glass. The intensity decreases weakly due to the decreasing intensity of the inelastic signal, while the elastic intensity is temperature independent.

The change in the nonergodicity factor with temperature in the glass is essentially governed by the temperature population factor of the phonons. Neither the speed of sound nor the frozen in fluctuations seen in the elastic intensity change significantly with temperature. This means that f_Q inevitably decreases as temperature increases in the glass. The pressure dependence is however more complicated. In most cases, pressure will decrease the frozen in fluctuations and at the same time increase the glassy modulus. These two effects will have an opposite effect on the nonergodicity factor. There is no *a priori* reason why one of them should be the dominant effect.

IV. DISCUSSION

Because of the very rich phenomenology associated to the glass transition, one often resorts to correlations among various experimental characteristics considered as important or universal to understand it. Most of the correlations, as we develop below, refer to the fragility defined originally by Angell.[37] They bring empirically together the way the system becomes viscous very close to its structural arrest at T_g and any other signatures of the glass transition or its potential consequences in the glassy state. Of course, a great caution should be taken in searching for correlations besides all the specific aspects due to the microscopic nature of various systems and all error bars on the extracted quantities.

A. Nonergodicity factor and fragility

1. The background of the correlation

The temperature dependence of the nonergodicity factor can, in the harmonic approximation, be described by $f_Q(T) = 1/(1+aT)$, where a is given by the eigenvectors and eigenvalues of the vibrational normal modes and the inherent structure structure factor.[1] In order to define a dimensionless parameter, α, to characterize the temperature dependence of the nonergodicity factor, Scopigno *et al.*[1] introduced a scaling with T_g,

$$f_Q(T) = \frac{1}{1+\alpha\frac{T}{T_g}}. \tag{7}$$

The temperature dependence predicted from the harmonic approximation is always found at low temperatures in the glass, and most often all the way up to T_g. The parameter α can therefore easily be extracted as the low temperature slope of $1/f_Q$ as a function of T/T_g (see, e.g., Fig. 10). By comparing ten different glass-forming systems with fragilities in the range 20–90, Scopigno *et al.*[1] found that α is proportional to the isobaric fragility m_P with $m_P = 135\alpha$. This relation suggests that the glassy state contains information about the dynamics of the liquid just above T_g.

If the linear dependence of $1/f_Q$ holds up to T_g, then there is a one to one correspondence between $f_Q(T_g)$ and α[7],

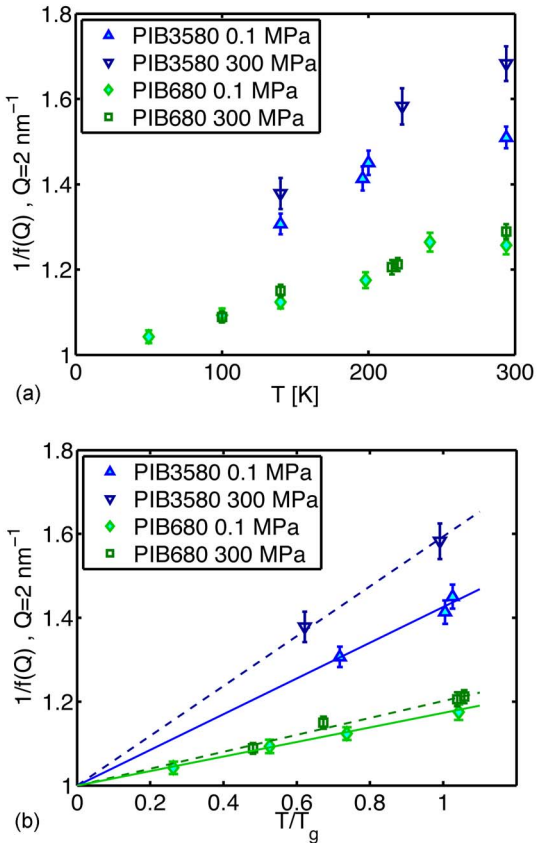

FIG. 10. (Color online) The inverse nonergodicity factor of PIB680 and PIB3580 as a function of temperature. (a) shows an absolute temperature scale, while (b) shows the temperature normalized to the pressure dependent glass transition temperature. The lines are fits to Eq. (7): the slope of the lines is equal to α.

$$f_Q(T_g) = \frac{1}{1+\alpha}. \tag{8}$$

This means that the correlation between fragility and α hints that there could be a correlation between $1/f_Q(T_g)$ and fragility, and this has also been verified for a number of glass formers.[7,11] However, the harmonic behavior is not always followed all the way up to T_g. Using α determined from low temperatures rather than from Eq. (8) is therefore not in general equivalent, and as the difference appears to be larger, the larger is the fragility.[38]

The nonergodicity factor is Q-independent in the low Q-region (see the previous section), and the result regards the nonergodicity factor in this low Q domain. Scopigno *et al.*[1] used $Q=2$ nm^{-1} as a reference Q-value when comparing different systems, and we follow this convention. The liquid is in thermodynamic equilibrium down to T_g and the low Q limit of $f_Q(T_g)$ is therefore determined by the high frequency adiabatic longitudinal compliance, $1/(\rho v_l^2)$ and the equilibrium isothermal compressibility [see Eq. (6)].

In the previous section we showed that this interpretation in terms of compressibilities appears to be relevant even at the relative high Q-value of 2 nm^{-1}. The same conclusion was drawn by Buchenau and Wischnewski.[7] In this frame the correlation can be expressed in the following way: the larger

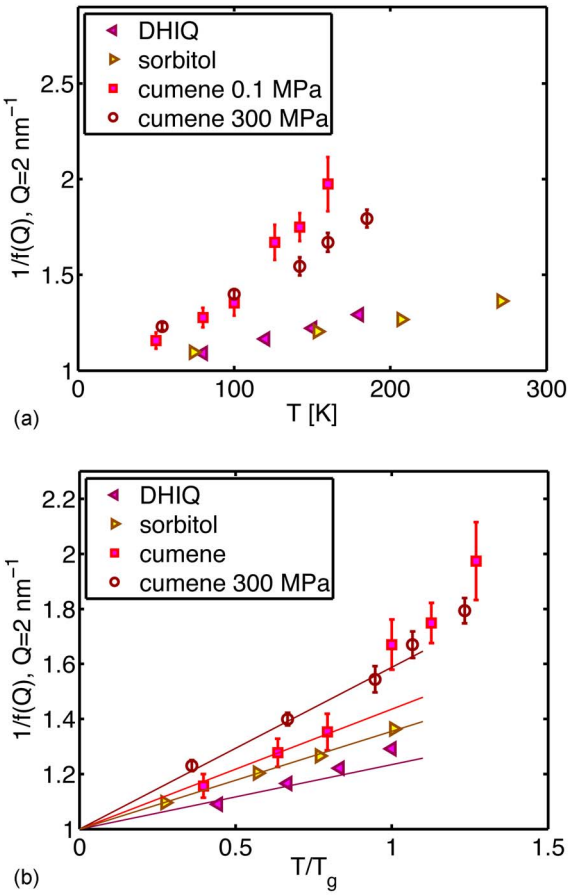

FIG. 11. (Color online) The inverse nonergodicity factor of cumene, DHIQ, and sorbitol as a function of temperature. (a) shows an absolute temperature scale, while (b) shows temperature normalized to the pressure dependent glass transition temperature. The lines are fits to Eq. (7) and the slope of the lines is equal to α.

the high frequency longitudinal compliance is, compared to the isothermal compressibility, the larger is the fragility.

2. Ambient pressure: Large range of fragility

Figure 10(a) shows the inverse nonergodicity factor of the PIB samples as a function of temperature. Note first of all that the $f_Q(T)=1/(1+aT)$ behavior is followed all the way up to T_g in this case, meaning that Eq. (8) is valid. Figure 10(b) shows the same data (excluding points above T_g) with the temperature scale normalized to the (molecular weight dependent) glass transition temperature. The slopes of the curves in Fig. 10(b) correspond to α, and it is clearly seen that α is larger for the larger molecular weight. We do not have the fragility of the samples at intermediate molecular weight, but the low molecular weight sample, PIB680, has fragility $m_P=70$,[30] while the high molecular PIB has a much lower fragility $m_P=46$.[19] Also Sokolov *et al.* found that PIB has decreasing fragility with increasing molecular weight.[39] The molecular weight dependence of α is thus opposite to what one expected from the correlation between α and fragility for this polymer. Figure 11 shows $1/f_q$ for the molecular liquids studied, cumene, sorbitol, and DHIQ. The slopes of the lines in Fig. 11(b) are fits to Eq. (8) and illustrate α. As mentioned, above, Eq. (8) only holds at low temperatures. In some cases particularly DHIQ and also cumene at atmospheric pressure, we see deviations from the low temperature behavior even well below T_g. Therefore we restrict the fit to the range where we can get a result staying within the error bars. It is clearly seen that the very fragile liquid DHIQ ($m_P=158$, the speed of sound 2750 m/s at $Q=2$ nm^{-1}) has a small α-value, at odds with the proposed correlation between α and m. Also the fragile sorbitol ($m_P=100$, the speed of sound 3830 m/s at $Q=2$ nm^{-1}) shows a clearly smaller slope α than the fragile glass-former cumene ($m_P=90$, the speed of sound 2600 m/s at $Q=2$ nm^{-1}). The collected values of isobaric fragility and our new results on α are shown in Fig. 12 along with earlier literature data. It is clearly seen that there is no one to one correspondence between fragility and α; one could at best say that there is a trend in the suggested direction.

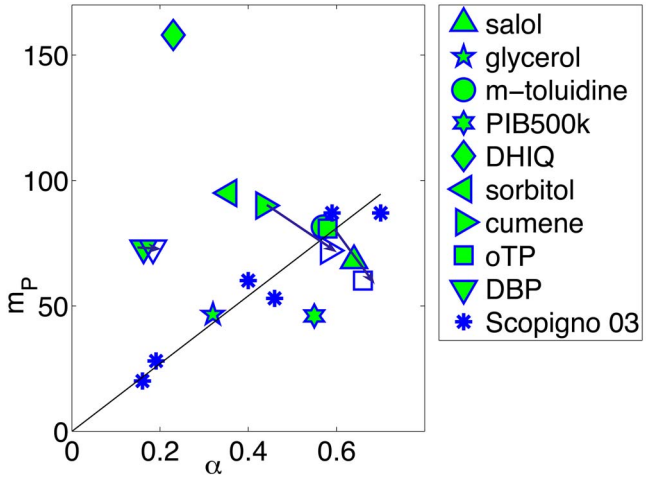

FIG. 12. (Color online) The isobaric fragility as a function of the parameter α for a number of different liquids. The full symbols are data at atmospheric pressure. The open symbols are data at elevated pressure (in the range of 200–300 MPa). The arrow shows the direction of increasing pressure. See Table II for references. The $*$ are data taken from Scopigno *et al.*(Ref. 1) these samples are not considered in Fig. 13 because the relevant data are not available.

3. Pressure

The isobaric fragility will in most glass formers decrease with increasing pressure. This is the case for cumene for which $m_p(P=0.1\ \text{MPa})=90$ while $m_p(P=300\ \text{MPa})=72$. The fragility is also expected to decrease with pressure in the case of the PIB samples because this is by far the most common behavior in polymers.[40]

We showed in Sec. III C that the nonergodicity factor at a given temperature is basically independent of pressure. However, the parameter α also involves a scaling with T_g, and T_g is in itself increasing with pressure. This has the consequence that α increases with pressure for all the samples we have studied. The pressure dependence of α and how it is related to the pressure dependence of T_g are illustrated in Figs. 10 and 11.

IXS spectra have been studied at elevated pressure for *ortho*-terphenyl (o-TP) by Monaco *et al.*[41] and dibutylphtalate (DBP) by Mermet *et al.*[42] It was found also in these cases that the nonergodicity factor is independent of pressure

when evaluated at a constant temperature. The pressure independence of the nonergodicity factor in the glassy phase hence appears to be general (in the considered pressure range <300 MPa). The glass transition temperature is always increasing with pressure and this means that a pressure independent nonergodicity factor leads to an increase in α. The isobaric fragility of DBP stays constant when going from atmospheric pressure up to 300 MPa. o-TP, on the other hand, is one of the examples where isobaric fragility decreases quite significantly.

The pressure dependence of α and isobaric fragility m_P have as mentioned in the introduction been studied in a molecular dynamics simulations of CKN by Ribeiro *et al.*[12] In this case it was also found that α increases with increasing pressure, which supports the hypothesis that α always increases with increasing pressure. Ribeiro *et al.*[12] found that the isobaric fragility m_P increases with increasing pressure. This behavior is somewhat uncommon but could be specific to this system or to the conditions of the simulation, e.g., the short time scale at which the fragility is evaluated.

The overall picture is that m_P can have different dependencies on pressure, decrease, increase, or stay constant, but the most common behavior is that it decreases. The parameter α, on the other hand, has been found to increase with pressure in all studied cases studied so far. This general behavior shows that the mechanisms responsible for the change in m_P with changing pressure do not have a signature in α. In Fig. 12 we show m_p as a function of α for a number of systems. We also include the available data at elevated pressure illustrating the above statement. However, it is also seen that the pressure induced changes in both m_P and α are limited in the pressure range used so far (200–300 MPa). The picture could be different at higher pressures.

4. Nonergodicity factor and the effect of density

The fragility considered by Scopigno *et al.* and in most similar studies is the isobaric fragility. The isobaric fragility is a measure of how much the temperature dependence of the relaxation time (or the viscosity) departs from the Arrhenius behavior when the sample is cooled under isobaric conditions.

The isobaric fragility is defined as

$$m_P = \left.\frac{\partial \log_{10}(\tau)}{\partial T_\tau/T}\right|_P \quad (T = T_\tau), \tag{9}$$

where the derivative is to be evaluated at T_τ. T_τ is defined as the temperature at which the relaxation time reaches the value τ, e.g., $\tau=100$ s.

However, when cooling under isobaric conditions two things happen at the same time: the thermal energy of the system decreases and the density increases. These two effects both contribute to the slowing down of the dynamics, and the isobaric fragility therefore contains information on both these effects.

The two effects can be formally separated by using the chain rule of differentiation:

$$m_P = \left.\frac{\partial \log_{10}(\tau)}{\partial T_\tau/T}\right|_\rho (T = T_\tau) + \left.\frac{\partial \log_{10}(\tau)}{\partial \rho}\right|_T \left.\frac{\partial \rho}{\partial T_\tau/T}\right|_P (T = T_\tau) \tag{10}$$

$$= m_\rho + \left.\frac{\partial \log_{10}(\tau)}{\partial \rho}\right|_T \left.\frac{\partial \rho}{\partial T_\tau/T}\right|_P (T = T_\tau), \tag{11}$$

where the second equality sign defines the isochoric fragility m_ρ and where both fragilities are evaluated at the same thermodynamic state point, e.g., at a given pressure P_1 defining $T_\tau(P_1)$.

Within the past decade a substantial amount of relaxation time and viscosity data has been collected at different temperatures and pressures/densities mainly by the use of dielectric spectroscopy. On the basis of the existing data, it is relatively well established that the temperature and density dependence of the relaxation time can be expressed as first suggested by Alba-Simionesco *et al.*,[21] as

$$\tau(\rho, T) = F\left(\frac{e(\rho)}{T}\right). \tag{12}$$

The function $e(\rho)$ defines an energy scale that is solely dependent on density. The result is empirical and has been supported by the work of several groups for a variety of glass-forming liquids and polymers.[14,21–23,40,43–45]

The scaling law has the formal consequence that the isochoric fragility is constant.[22,24] That is, m_ρ will have the same value at different densities when evaluated at the same relaxation time (and consequently at a different temperature). A second consequence of the scaling law is that the isobaric fragility can be rewritten as

$$m_P = m_\rho\left(1 + \alpha_P T_\tau \frac{d \log e(\rho)}{d \log \rho}\right), \tag{13}$$

where m_P and m_ρ are again evaluated at a given relaxation time τ and α_P is the isobaric expansion coefficient.

This expression illustrates that the relative effect of density on the slowing down upon isobaric cooling, i.e., the second term in the parentheses, can be decomposed into two parts: the temperature dependence of the density measured by $T_\tau\alpha_P = -\partial \log \rho / \partial \log T|_P$ $(T=T_\tau)$ and the density dependence of the activation energy, which is contained in $d \log e(\rho)/d \log \rho$.

Since m_ρ is constant along an isochrone, it follows from Eq. (13) that the change in m_P with increasing pressure is due to the change in $\alpha_P T_\tau d \log e(\rho)/d \log \rho$. T_τ increases with pressure, $\alpha_P T_\tau(P)$ decreases, whereas $d \log e(\rho)/d \log \rho = x$ is often to a good approximation constant in the range of densities accessible. The most common behavior seen from the data compiled by Ronald *et al.*[40] is that the isobaric fragility decreases or stays constant with pressure, with few exceptions. This indicates that the decrease in $\alpha_P T_g(P)$ usually dominates over the other factors.

From the previous section it was seen that the parameter α does not follow the pressure dependence of the fragility. From the above considerations we see that this means that

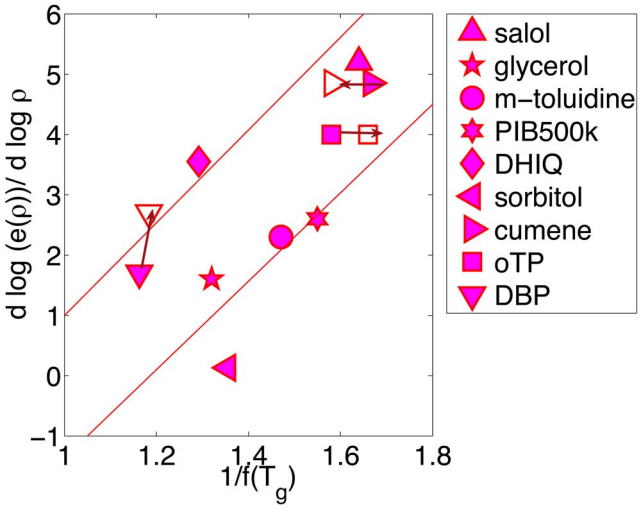

FIG. 13. (Color online) The value of $d\log e/d\log\rho$ as a function of the inverse nonergodicity factor for a number of different liquids. The full symbols are data at atmospheric pressure. The open symbols are data at elevated pressure (in the range of 200–300 MPa). The arrow shows the direction of increasing pressure. The lines are guides to the eyes. See Table II for references.

the parameter α is unrelated to $\alpha_P T_g(P)$, which is the term responsible for the pressure dependence of the fragility.

Based on a comparison between the terms in the decomposition in Eq. (13) and the nonergodicity factor at T_g, it was suggested by two of us[13] that the original correlation found between α and m_P might be a reminiscent signature of a more fundamental relation between $1/f_Q(T_g)$ and the effect of density on the relaxation time [recall that $1/f_Q(T_g)=\alpha+1$ if the harmonic behavior is followed up to T_g]. We suggested that $1/f_Q(T_g)$ might be correlated to either $d\log e(\rho)/d\log\rho$ or to $\alpha_P T_g d\log e(\rho)/d\log\rho$. It was not possible to distinguish the quality of these two suggested correlations from the data presented in Ref. 13.

The term $\alpha_P T_g d\log e(\rho)/d\log\rho$ governs the pressure dependence of m_P and it is as mentioned above decreasing with increasing pressure. $1/f_Q(T_g)$, on the other hand, is either increasing or close to constant. Thus $1/f_Q(T_g)$ and $\alpha_P T_g d\log e(\rho)/d\log\rho$ have opposite dependence of pressure.

Considering $1/f_Q(T_g)$ and $d\log e(\rho)/d\log\rho$, on the other hand, the qualitative behavior is the same for both quantities; we find values that are either close to constant or increasing with pressure. This is illustrated in Fig. 13. The two parameters $1/f_Q(T_g)$ and $d\log e(\rho)/d\log\rho$ appear to be weakly correlated, although it is a trend rather than a clear one to one correspondence.

Nevertheless, by comparing Figs. 12 and 13, and especially by considering the pressure dependences, we conclude that if there is a correlation holding some information about a connection between fast dynamics and viscous slowing down, it is most likely to be a correlation between $d\log e(\rho)/d\log\rho$ and $1/f_q(T_g)$. It is unclear what the interpretation of such a correlation could be. $d\log e(\rho)/d\log\rho$ is a measure of the density dependence of the characteristic energy $e(\rho)$. Thus, the correlation means that $e(\rho)$ is very density dependent when $1/f_q(T_g)$ is large. $1/f_q(T_g)$ is large if the vibrational contribution to the compressibility is large. Or put in other words $1/f_q(T_g)$ is large when the nonrelaxing part of the volume changes are large relative to the relaxing part of the volume changes. A relation between $1/f_q(T_g)$ and $d\log e(\rho)/d\log\rho$ therefore indicates that the vibrational part of the volume changes has a stronger influence on $e(\rho)$ than the relaxational part of the volume changes.

B. Nonergodicity factor and thermodynamic fragility

Some experimental features are considered as a characteristic and important inputs for theories; the predictions of those theories can, in turn, be tested by experiments. The correlations we are interested in may help in selecting these characteristic features, but the correlations are always empirically established; they denote tendencies and come out from the input of a large number of systems, but a one to one correspondence never holds. The nonergodicity factor is one of the crucial parameters to which a lot of attention was devoted in the past because it is a central quantity in the mode coupling theory. In their original work, Scopigno *et al.*[1] proposed to correlate the temperature dependence of the nonergodicity factor deep in the glassy state with the temperature dependence of the relaxation time in the supercooled liquid, assuming that the vibrational and the relaxational processes present a clear separation in time (an assumption valid up to T_g as soon as no extra processes play a role). As we have shown in the previous section, the correlation does not hold anymore when pressure is applied. However, as explained above, taken at T_g the nonergodicity factor characterizes the amplitude of the structural relaxation when ergodicity is macroscopically broken and it is appealing to think that it carries particular features of the viscous liquid into the glassy state. We found that the amplitude of the α-process, as measured by $f_Q(T_g)$, is unlikely to be correlated with the temperature dependence of the α-process; however, the correlation between $f_Q(T_g)$ and other characteristics of the glass transition could still be justified. We have therefore checked the validity of the correlation via other experimental aspects associated to the fragility. The results are preliminary because there are very few samples for which all the relevant data are available. Therefore we do not show figures in illustrating the points of the following sections, as each figure would contain only 4 or 5 points.

A natural link is often proposed between the thermodynamics and the kinetics of supercooled liquids through the glass transition where the heat capacity at constant pressure drops upon cooling. Thus the temperature dependence of the relaxation times (or the viscosity) is compared to the rate at which the excess entropy of the liquid over the crystalline phase changes as T_g is approached. By establishing such a link, Adam and Gibbs related the increase in the relaxation times and the rapid decrease in the configurational entropy,[46] which is approximated experimentally by the excess entropy of the liquid relative to the crystal.

In our attempt to compare $f_Q(T_g)$ with other quantities, we have not found any consistent relation between $f_Q(T_g)$ and the residual excess entropy at T_g nor with the heat capacity jumps (normalized to the heat capacity of the glass or

to the number of beads[25,26,47]). Furthermore, in that framework, a thermodynamic fragility is defined as the ratio between the amplitude of the heat capacity jump at T_g and the melting entropy;[20] it is found for nonpolymeric systems as being proportional to the kinetic one. Here again, and consistently with our findings, no correlation between $f_Q(T_g)$ and the thermodynamic fragility is found. This suggests that there is no simple way to link the density fluctuations frozen in at T_g and the characteristic features of the glass transition seen in the heat capacity.

Another aspect characterizing the glass transition is the temporal behavior of the relaxation function describing the response to a perturbation; it is known to exhibit nonexponential behavior, which is often associated to the existence of spatially heterogeneous domains, also called, in the context of the above mentioned Adam–Gibbs theory, cooperatively rearranging regions. Therefore, since $f_Q(T_g)$ reflects the amplitude of the α-process and how closely the molecules are trapped in the cage formed by the neighbors, its relation to the existence and the size of dynamical heterogeneities could be addressed. Unfortunately, the size of these domains is not easily extracted and their existence can be questioned. Instead, an estimate of the number of molecules dynamically correlated, N_{corr},[48,49] was recently proposed. However, we find no correlation between $f_Q(T_g)$ and N_{corr} either. Thus, $f_Q(T_g)$ refers to how closely the molecules are trapped in the cage formed by the neighbors, but not to how many of them are dynamically correlated.

Other phenomenological definitions of fragility, e.g., $D, F_{1/2}$ (see Ref. 50) and other possible correlations to short-time properties could be checked as well. This list is, of course, not exhaustive, but our successive attempts lead to the same conclusion: absence of or weak correlation between the fragility and the nonergodicity factor at T_g or its temperature dependence deep in the glass.

C. Broadening of the acoustic excitations

Another high frequency property, which has recently been proposed to relate to the fragility, and hereby to the viscous slowing down, is the broadening of the acoustic excitations. The proposal is that strong systems have large broadening of the acoustic excitations,[27] with the broadening measured in terms of the low Q limit of the value Γ/Q^2. The larger broadening in strong systems could be related to the higher boson peak intensity, which also appears to be found in strong systems:[4] both the damping and the boson peak intensity would then be a signature of either structural disorder or fluctuating elastic constants.[51]

From our data we have seen that Γ is essentially independent of pressure in cumene, while the isobaric fragility slightly decreases as a function of pressure. We have reported this and all other available data in Fig. 14. It is seen that though the available values actually agree with the behavior expected based on the proposed correlation,[27] the dependence of Γ/Q^2 on fragility flattens out at high fragilities. That is, broadening of the acoustic excitation appears to become independent of fragility for values of m_p higher than 50.

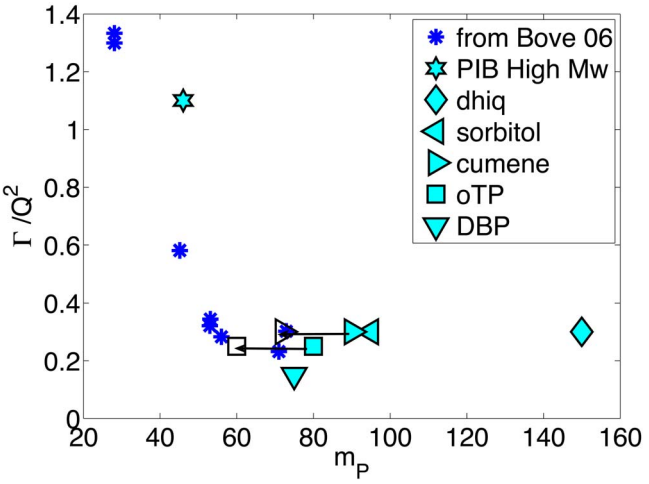

FIG. 14. (Color online) The broadening of the acoustic excitation Γ over Q^2 as a function of isobaric fragility for a number of different glass formers. The $*$ shows data taken from Bove *et al.* (Ref. 27). The open symbols show data at elevated pressure (in the range of 200–300 MPa). The direction of the arrow indicates increasing pressure. See Table II for references.

V. CONCLUSIONS

We have studied the coherent dynamical structure factor by using IXS for a series of polymer and molecular liquids whose fragilities at T_g are extended up to the highest values reported in literature. Moreover we have proposed to control the change in fragility by introducing new parameters such as pressure or molecular weight in the case of polymers. Thus we have been able to scrutinize some of the relations between the temperature dependence of the viscous slowing down in the liquid and the fast dynamics in the liquid or the glass. This gives more controlled information than that obtained from the traditional route of comparing chemically different systems.

The IXS data have been collected both above and below the glass transition temperature. The general picture is that while the speed of sound shows the expected increase with increasing pressure, the broadening of the acoustic excitation and the nonergodicity factor are essentially pressure independent within the pressure range we have accessed. We find that the increase in molecular weight in the particular case of PIB leads to an increase in the speed of sound and a decrease in the nonergodicity factor. However, this latter trend should be confirmed on other polymers and more work is still required in that direction.[34]

We have compared the results obtained to the proposed correlation between isobaric fragility and the parameter α, which is extracted from the temperature dependence of the nonergodicity factor in the glassy state.[1] We find that the pressure and molecular weight dependences of α are opposite to that expected from the suggested correlation to isobaric fragility. This clearly shows that the parameter α does not hold information on the mechanisms that are governing the pressure and molecular weight dependence of the isobaric fragility. We also consider a related correlation which has been suggested to exist between the inverse of the nonergodicity factor at the glass transition $1/f_q(T_g)$ and the parameter $d\log e/d\log\rho$, which describes how density

changes the activation energy associated with the α-relaxation. We find qualitative agreement between the pressure dependence of $1/f_q(T_g)$ and $d\log e/d\log\rho$, while the quantitative agreement is less convincing. It is thus still an open question whether there is any intimate relation between the rate of the viscous slowing and the vibrational properties contained in the nonergodicity factor.

Lastly we briefly compare our findings to the recently proposed correlation between isobaric fragility and the broadening of the acoustic excitations.[27] While the correlation works apparently well for strong systems ($m_P<50$) including our results on high M_w PIB, it does not hold for highly fragile liquids. For these systems, in fact, the broadening of the acoustic exitations is almost independent of fragility.

The establishment of correlations between fragility measured around T_g and glassy properties at low temperatures is not a straightforward task. This does not mean that the glassy properties do not originate from those of the supercooled liquid. However, in this work we were not able to enlighten such a relation by crosschecking with additional parameters possible correlations between the nonergodicity factor in the glass and the temperature dependence of the relaxation time in the liquid.

ACKNOWLEDGMENTS

This work was supported by the CNRS (France) and Grant No. 645-03-0230 from Forskeruddannelsesrådet (Denmark). We thank Bo Jakobsen, Michael Krisch, Alexandre Beraud, and Roberto Verbeni for their practical help and Tullio Scopigno for many inspiring discussions.

[1] T. Scopigno, G. Ruocco, F. Sette, and G. Monaco, Science **302**, 849 (2003).
[2] V. N. Novikov and A. P. Sokolov, Nature (London) **431**, 961 (2004).
[3] K. L. Ngai, Philos. Mag. **84**, 1341 (2004).
[4] A. P. Sokolov, E. Rössler, A. Kisliuk, and D. Quitmann, Phys. Rev. Lett. **71**, 2062 (1993).
[5] A. P. Sokolov, R. Calemczuk, B. Salce, A. Kisliuk, D. Quitmann, and E. Duval, Phys. Rev. Lett. **78**, 2405 (1997).
[6] J. C. Dyre and N. B. Olsen, Phys. Rev. E **69**, 042501 (2004).
[7] U. Buchenau and A. Wischnewski, Phys. Rev. B **70**, 092201 (2004).
[8] U. Buchenau and R. Zorn, Europhys. Lett. **18**, 523 (1992).
[9] J. C. Dyre, Nature **3**, 749 (2004).
[10] J. C. Dyre, Rev. Mod. Phys. **78**, 953 (2006).
[11] V. N. Novikov, Y. Ding, and A. P. Sokolov, Phys. Rev. E **71**, 061501 (2005).
[12] M. C. C. Ribeiro, T. Scopigno, and G. Ruocco, J. Chem. Phys. **128**, 191104 (2008).
[13] K. Niss and C. Alba-Simionesco, Phys. Rev. B **74**, 024205 (2006).
[14] K. Niss, C. Dalle-Ferrier, G. Tarjus, and C. Alba-Simionesco, J. Phys.: Condens. Matter **19**, 076102 (2007).
[15] K. Niss, B. Frick, J. Ollivier, A. Beraud, A. Sokolov, B. Begen, V. Novikov, and C. Alba-Simionesco, Phys. Rev. Lett. **99**, 055502 (2007).
[16] B. Begen, A. Kisliuk, V. Novikov, A. Sokolov, K. Niss, A. Chauty-Cailliaux, C. Alba-Simionesco, and B. Frick, J. Non-Cryst. Solids **352**, 041510 (2006).
[17] B. Frick and C. Alba-Simionesco, Appl. Phys. A: Mater. Sci. Process. **74**, S549 (2002).
[18] B. Frick, G. Dosseh, A. Cailliaux, and C. Alba-Simionesco, Chem. Phys. **292**, 311 (2003).
[19] Y. F. Ding, V. N. Novikov, A. P. Sokolov, A. Cailliaux, C. Dalle-Ferrier, C. Alba-Simionesco, and B. Frick, Macromolecules **37**, 9264 (2004).
[20] L. M. Wang, C. A. Angell, and R. Richert, J. Chem. Phys. **125**, 074505 (2006).
[21] C. Alba-Simionesco, D. Kivelson, and G. Tarjus, J. Chem. Phys. **116**, 5033 (2002).
[22] G. Tarjus, D. Kivelson, S. Mossa, and C. Alba-Simionesco, J. Chem. Phys. **120**, 6135 (2004).
[23] R. Casalini and C. M. Roland, Phys. Rev. E **69**, 062501 (2004).
[24] C. Alba-Simionesco and G. Tarjus, J. Non-Cryst. Solids **352**, 4888 (2006).
[25] V. Lubchenko and P. G. Wolynes, J. Chem. Phys. **119**, 9088 (2003).
[26] J. D. Stevenson and P. G. Wolynes, J. Phys. Chem. B **109**, 1503 (2005).
[27] L. E. Bove, C. Petrillo, A. Fontana, A. Ivanov, C. Dreyfus, and A. P. Sokolov, Physica B **385**, 16 (2006).
[28] URL http://www.esrf.eu/UsersAndScience/Experiments/HRRS/ID16/
[29] A. Chauty-Cailliaux, Ph.D. thesis, Université Paris 11, Ursay, France, 2003.
[30] K. Niss, Ph.D. thesis, Université Paris 11, Orsay, France, 2007.
[31] G. Ruocco and F. Sette, J. Phys.: Condens. Matter **13**, 9141 (2001).
[32] B. Farago, A. Arbe, J. Colmenero, R. Faust, U. Buchenau, and D. Richter, Phys. Rev. E **65**, 051803 (2002).
[33] L. E. Bove, F. Formisano, E. Guarini, A. Ivanov, C. Petrillo, and F. Scchett, J. Non-Cryst. Solids **353**, 3139 (2007).
[34] C. Dalle-Ferrier (unpublished).
[35] M. Fuchs and A. Latz, J. Chem. Phys. **95**, 7074 (1991).
[36] I. C. Sanchez and J. Cho, Polymer **36**, 2929 (1995).
[37] C. A. Angell, J. Non-Cryst. Solids **131**, 13 (1991).
[38] T. Scopigno, personal communication (March 2007).
[39] A. P. Sokolov, V. N. Novikov, and Y. Ding, J. Phys.: Condens. Matter **19**, 205116 (2007).
[40] C. M. Roland, S. Hensel-Bielowska, M. Paluch, and R. Casalini, Rep. Prog. Phys. **68**, 1405 (2005).
[41] A. Monaco, Ph.D. thesis, Université J. Fourier de Grenoble, Grenoble, France, 2006.
[42] A. Mermet, E. Duval, A. Polian, and M. Krisch, Phys. Rev. E **66**, 031510 (2002).
[43] C. Dreyfus, A. L. Grand, J. Gapinski, W. Steffen, and A. Patkowski, Eur. Phys. J. B **42**, 309 (2004).
[44] A. Reiser, G. Kasper, and S. Hunklinger, Phys. Rev. B **72**, 094204 (2005).
[45] G. Floudas, K. Mpoukouvalas, and P. Papadopoulos, J. Chem. Phys. **124**, 074905 (2006).
[46] G. Adam and J. H. Gibbs, J. Chem. Phys. **43**, 139 (1965).
[47] V. Privalko, J. Chem. Phys. **84**, 3307 (1980).
[48] L. Berthier, G. Biroli, J. P. Bouchaud, L. Cipelletti, D. E. Masri, D. L'hote, F. Ladieu, and M. Perino, Science **310**, 1797 (2005).
[49] C. Dalle-Ferrier, C. Thibierge, C. Alba-Simionesco, L. Berthier, G. Biroli, J. P. Bouchaud, F. Ladieu, D. L'Hote, and G. Tarjus G, Phys. Rev. E **76**, 011507 (2007).
[50] R. Richert and C. A. Angell, J. Chem. Phys. **108**, 9016 (1998).
[51] W. Schirmacher, G. Ruocco, and T. Scopigno, Phys. Rev. Lett. **98**, 025501 (2007).
[52] G. Li, H. E. King, W. F. Oliver, C. A. Herbst, and H. Z. Cummins, Phys. Rev. Lett. **74**, 2280 (1995).
[53] K. Niss, B. Jakobsen, and N. B. Olsen, J. Chem. Phys. **123**, 234510 (2005).
[54] R. Richert, K. Duvvuri, and L. T. Duong, J. Chem. Phys. **118**, 1828 (2003).
[55] N. B. Olsen, J. Non-Cryst. Solids **235–237**, 399 (1998).
[56] D. J. Plazek and K. L. Ngai, Macromolecules **24**, 1222 (1991).
[57] A. J. Barlow, J. Lamb, and A. J. Matheson, Proc. R. Soc. London, Ser. A **292**, 322 (1966).
[58] L. T. Minassian, K. Bouzar, and C. Alba, J. Phys. Chem. **92**, 487 (1988).
[59] A. C. Ling and J. E. Willard, J. Phys. Chem. **72**, 3349 (1968).
[60] P. W. Bridgman, Proc. Am. Chem. Soc. **77**, 129 (1949).
[61] W. T. Laughlin and D. R. Uhlmann, J. Phys. Chem. **76**, 2317 (1972).
[62] M. Paluch, K. L. Ngai, and S. Hensel-Bielowka, J. Chem. Phys. **114**, 10872 (2001).
[63] C. M. Roland, M. Paluch, T. Pakula, and R. Casalini, Philos. Mag. **84**, 1573 (2004).
[64] C. Alba-Simionesco, A. Cailliaux, A. Alegria, and G. Tarjus, Europhys. Lett. **68**, 58 (2004).

[65] N. O. Birge, Phys. Rev. B **34**, 1631 (1986).
[66] A. Mandanici, M. Cutroni, and R. Richert, J. Chem. Phys. **122**, 084508 (2005).
[67] C. Alba-Simionesco, J. Fan, and C. A. Angell, J. Chem. Phys. **110**, 5262 (1999).
[68] L. Comez, S. Corezzi, G. Monaco, R. Verbeni, and D. Fioretto, Phys. Rev. Lett. **94**, 155702 (2005).
[69] R. Casalini, K. J. McGrath, and C. M. Roland, J. Non-Cryst. Solids **352**, 4905 (2006).
[70] P. K. Dixon and S. R. Nagel, Phys. Rev. Lett. **61**, 341 (1988).
[71] D. H. Huang and G. B. McKenna, J. Chem. Phys. **114**, 5621 (2001).
[72] A. Tölle, H. Schober, J. Wuttke, O. G. Randl, and F. Fujara, Phys. Rev. Lett. **80**, 2374 (1998).
[73] C. Dreyfus, A. Aouadi, J. Gapinski, M. Matos-lopes, W. Steffen, A. Patkowski, and R. M. Pick, Phys. Rev. E **68**, 011204 (2003).
[74] D. Fioretto, U. Buchenau, L. Comez, A. Sokolov, C. Masciovecchio, A. Mermet, G. Ruocco, F. Sette, L. Willner, B. Frick, D. Richter, and L. Verdini, Phys. Rev. E **59**, 4470 (1999).